Physical and biogeochemical regionalisations and climate velocities in the epipelagic and mesopelagic Southern Indian Ocean

C. Merland[1,2,3]✉, C. Azarian[1,4]✉, F. d'Ovidio[1]✉ and C. Cotté[1]✉

[1] Oceanography and Climate Laboratory: Experiments and Numerical Approaches (LOCEAN-IPSL). Sorbonne Université, CNRS, IRD, MNHN
4 place Jussieu, 75005 Paris
France

[2] IFREMER Centre Manche / mer du Nord
150 quai Gambetta. 62220 Boulogne sur Mer
France

[3] Institut de la Mer de Villefranche-sur-Mer (IMEV)
181 Chemin du Lazaret, 06230 Villefranche-sur-Mer
France

[4] Ecole Nationale des Ponts et Chaussées (ENPC),
Champs-sur-Marne
France.

Email: camille.merland@imev-mer.fr
clara.azarian@locean.ipsl.fr
francesco.dovidio@locean.ipsl.fr
cedric.cotte@locean.ipsl.fr

Abstract

Environmental regionalisations are useful tools for spatial planning and are mostly performed at the global scale to define biogeochemical provinces from surface data or in the mesopelagic zone. However, these regionalisations often lack separations at scales relevant for conservation as they do not always consider regional patterns such as island effects or regional dynamic patterns. Our study aimed to overcome these limitations by defining coherent physical and biogeochemical regions within the Southern Indian Ocean (20°W-160°E; 30°S-60°S), considering both spatial and temporal dynamics of environmental parameters. For this purpose, two complementary approaches have been used: one focusing on surface environmental data, and the other considering space-time dimensions through their vertical profiles. The first classical method, based on multivariate analyses, allowed us to delineate regions latitudinally due to the existing temperature and oxygen concentration gradient and revealed regional patterns such as highly energetic regions or productive areas. The newly developed second approach used functional analyses and provided additional information, including subdivision in the Subtropical Zone dominated by mesopelagic patterns. This subdivision results from temperature differences. It separates longitudinally the subtropical region with warmer waters found in the western area, likely transported from lower latitudes by the Agulhas Return Current. Climate velocities of temperature (i.e. speed of isotherm drift) were also computed for both epipelagic and mesopelagic regions to investigate their potential shift due to climate change. This environmental regionalisation brings relevant information to understand the distribution of the pelagic diversity and abundance and highlights the importance of accounting for vertical structures in a context of climate change.

Résumé

Les régionalisations environnementales sont des outils utiles pour l'aménagement du territoire. Elles sont principalement réalisées à l'échelle mondiale afin de définir des provinces biogéochimiques à partir de données de surface ou dans la zone mésopélagique. Cependant, ces régionalisations manquent souvent de séparation à des échelles pertinentes pour la conservation, car elles ne tiennent pas toujours compte des modèles régionaux tels que les effets insulaires ou les modèles dynamiques régionaux. Notre étude visait à surmonter ces limites en définissant des régions physiques et biogéochimiques cohérentes dans le sud de l'océan Indien (20° O-160° E ; 30° S-60° S), en tenant compte à la fois de la dynamique spatiale et temporelle des paramètres environnementaux. À cette fin, deux approches complémentaires ont été utilisées : l'une axée sur les données environnementales de surface, l'autre tenant compte des dimensions spatio-temporelles à travers leurs profils verticaux. La première méthode classique, basée sur des analyses multivariées, nous a permis de délimiter des régions latitudinalement en fonction du gradient de température et de concentration en oxygène existant et a révélé des schémas régionaux tels que des régions à forte énergie ou des zones productives. La deuxième approche, récemment mise au point, a utilisé des analyses fonctionnelles et a fourni des informations supplémentaires, notamment une subdivision en zone subtropicale dominée par des schémas mésopélagiques. Cette subdivision résulte des différences de température. Il sépare longitudinalement la région subtropicale aux eaux plus chaudes située dans la partie occidentale, probablement transportées depuis des latitudes plus basses par le courant de retour des Aiguilles. Les vitesses climatiques de la température (c'est-à-dire la vitesse de dérive des isothermes) ont également été calculées pour les régions épipélagiques et mésopélagiques afin d'étudier leur déplacement potentiel en raison du changement climatique. Cette régionalisation environnementale apporte des informations pertinentes pour comprendre la répartition de la diversité et de l'abondance pélagiques et souligne l'importance de prendre en compte les structures verticales dans un contexte de changement climatique.

Абстракт

Экологическая регионализация является эффективным инструментом для пространственного планирования и в основном проводится в глобальном масштабе для определения биогеохимических провинций на основе данных о поверхности или о мезопелагической зоне. Однако такие региональные классификации часто не учитывают различия в масштабах, значимых для охраны природы, поскольку не всегда принимают во внимание региональные особенности, такие как островной эффект или динамические процессы в регионе. Данное исследование направлено на преодоление указанных ограничений путем определения согласованных физических и биогеохимических регионов в южной части Индийского океана (20° з.д. – 160° в.д.; 30° ю.ш. – 60° ю.ш.), с учетом как пространственной, так и временной динамики экологических параметров. Для достижения этой цели были использованы два взаимодополняющих подхода: один фокусировался на данных о состоянии окружающей среды у поверхности, а другой учитывал пространственно-временные параметры по вертикальным срезам. Первый классический метод, основанный на многомерном анализе, позволил нам разграничить регионы по широтным координатам на основе существующего градиента температуры и концентрации кислорода и выявить региональные закономерности, такие как высокоэнергетические регионы или продуктивные зоны. Второй подход, разработанный недавно, использовал функциональный анализ и предоставил дополнительную информацию, включая подразделение на субтропическую зону, в которой преобладают мезопелагические закономерности. Это деление обусловлено разницей температур. Оно разделяет в продольном направлении субтропическую зону, при этом более теплые воды обнаруживаются в западной части, которые, вероятно, переносятся из более низких широт Обратным течением мыса Агульяс. Климатические темпы изменения температуры (т. е. скорость дрейфа изотерм) были также рассчитаны для эпипелагической и мезопелагической зон с целью изучения

их потенциального сдвига в результате изменения климата. Эта экологическая регионализация предоставляет важную информацию для понимания распределения пелагического разнообразия и численности и подчеркивает важность учета вертикальных структур в контексте изменения климата.

Resumen

Las regionalizaciones medioambientales son herramientas útiles para la planificación espacial y se realizan sobre todo a escala mundial con el objetivo de definir provincias biogeoquímicas a partir de datos de superficie o de la zona mesopelágica. Sin embargo, estas regionalizaciones no suelen estar definidas a escalas relevantes para la conservación, ya que no suelen tener en cuenta pautas regionales como los efectos de las islas o dinámicas regionales. Nuestro estudio tiene por objetivo superar estas limitaciones definiendo regiones físicas y biogeoquímicas coherentes dentro del Océano Índico Meridional (20°O-160°E; 30°S-60°S), teniendo en cuenta las dinámicas espaciales y temporales de los parámetros medioambientales. Para ello, se utilizan dos enfoques complementarios: uno centrado en los datos medioambientales de la superficie y otro que considera las dimensiones espacio-temporales en sus perfiles verticales. El primer método, convencional, basado en análisis multivariantes, permite delimitar regiones latitudinalmente gracias al gradiente de temperatura y de concentración de oxígeno existente y a pautas regionales como regiones altamente energéticas o áreas de alta productividad. El segundo enfoque, recientemente desarrollado, utiliza análisis funcionales e información adicional, incluida la subdivisión del sector Subtropical por pautas mesopelágicas. La razón de esta subdivisión son las diferencias de temperatura. Se observa una separación longitudinal, demarcándose una región subtropical occidental, con aguas más cálidas que probablemente son transportadas desde latitudes más bajas por la corriente de retorno de Agulhas. También se calcularon las velocidades climáticas (la velocidad de deriva de las isotermas) para las regiones epipelágica y mesopelágica con el fin de estudiar su posible desplazamiento debido al cambio climático. Esta regionalización medioambiental aporta información relevante para comprender la distribución de la diversidad y la abundancia pelágicas y pone de relieve la importancia de tener en cuenta las estructuras verticales en un contexto de cambio climático.

Introduction

Regionalisation is the process of identifying and mapping regions based on similar physical and/or biological factors (Vierros et al., 2009; Koubbi et al., 2011). This process aims to provide a better understanding of marine ecosystems and to support the definition of priority areas for conservation (Testa et al., 2021). However, defining regions at a large scale only based on biological factors is difficult in remote and data-limited regions. Instead, it is possible to conduct physical and biogeochemical regionalisation by partitioning the ocean according to defined environmental variables available for the entire domain and which are key for ecosystems (Grant et al., 2006).

Physical and biogeochemical regionalisations have been done in the past on a global scale, notably to define biogeochemical provinces by considering only the epipelagic zone (Longhurst, 2007), or only the mesopelagic zone (Reygondeau et al., 2018). However, in the Southern Ocean, regionalisations have mostly been dominated by the influence of bathymetry and sea ice extent, overlooking the importance of water masses dynamics (Raymond, 2014), or have been focused on particular domains, often not accounting for the transition with the Subtropical Zone (Godet et al., 2020). Moreover, as those regionalisations do not systematically consider regional patterns such as island effects or hydrodynamic zones (circulation, bathymetry-induced processes), they can also overlook finer scale boundaries between pelagic habitats.

Regionalisations generally provide mean habitat distributions at past and present times which can be modified by climate change. Climate change may yet alter boundaries of provinces and/or new habitats could emerge (Reygondeau et al., 2020). Climate velocity (i.e. the speed and direction at which isotherms drift due to climate change) can be a useful tool to quantify potential habitat shifts at scales relevant for conservation (Loarie et al., 2009; Brito-Morales et al., 2020). This metric has been applied in the Southern Indian Ocean, showing a spatial heterogeneity of isotherm drift speeds, despite a general southward shift of temperature conditions both in the epipelagic and mesopelagic layers under a high and a modest mitigation scenario by the end of the century (Azarian et al., 2023).

This work aims to delineate physical-biogeochemical regions to describe the environmental structuring and the main pattern of variability of the Southern Indian Ocean for pelagic organisms. To address this purpose, we propose to adopt two complementary approaches, a ‘classical’ approach focusing on surface environmental data and a newly developed functional three-dimensional approach (Pauthenet et al., 2018). Finally, the mean climate velocity for each of the physical-biogeochemical regions obtained is computed based on climate model projections under different emission scenarios to investigate their potential shift under climate change.

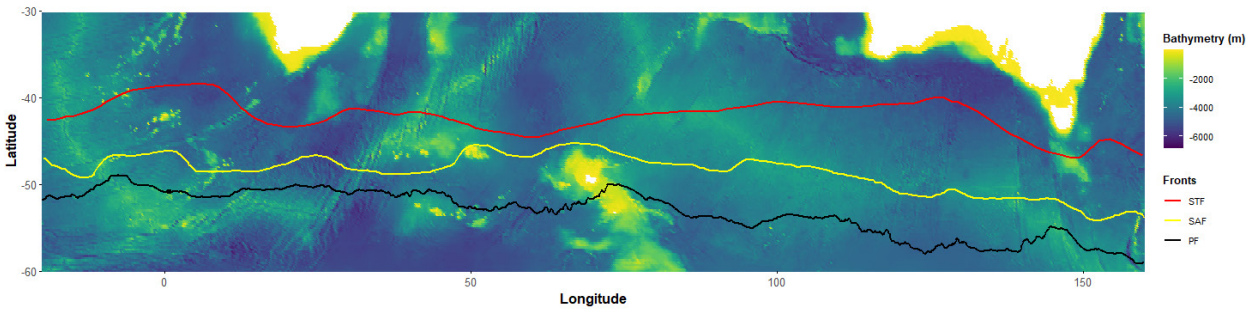

Figure 1: Map of the geographical areas studied showing the position of the different oceanic fronts

Material and methods

Study area

Our study area extends from 20°W to 160°E and from 30°S to 60°S (Figure 1), and defined as the region of interest for pelagic spatial planning (Makhado et al., 2019). This geographical region is marked by the presence of the Antarctic Circumpolar Current (ACC), the main physical driver of the Southern Ocean, and the different associated fronts. From north to south lay the Subtropical Front (STF) which defines the southern limit of warm and oligotrophic waters defining the subtropical gyre (Godet et al., 2020), the Subantarctic Front (SAF) and the Antarctic Polar Front (PF). The position of these fronts allows delineations of specific zones within the Southern Ocean: the Antarctic Zone (AZ), located to the south of the PF, the Polar Frontal Zone (PFZ) positioned between the PF and the SAF, the Subantarctic Zone (SAZ) positioned between the SAF and the STF, and the Subtropical Zone (STZ), located to the north of the STF.

Environmental data

Seasonal and monthly climatologies spanning 2009 to 2019 were constructed from environmental data parameters including temperature, salinity, chlorophyll concentration, oxygen concentration, mixed layer depth and kinetic energy (Table 1). These data come from the reanalysis 'Glorys' delivered by Mercator Ocean, which integrates both satellite and in situ data, available on the Marine Copernicus data portal (https://www.copernicus.eu). An ocean reanalysis provides a coherent time series of oceanic properties enabling the understanding and tracking of their evolution over time (Vidar et al., 2011; Ferry et al., 2012). The reanalysis provides monthly averages with a ¼ degree resolution grid that captures the temporal dynamics of the environment as certain parameters exhibit strong seasonality (chlorophyll concentration, mixed-layer depth, etc.).

Table 1: Description of the environmental parameters used in this work.

Environmental parameters	Abbreviation	Source and product	Spatial resolution	Temporal resolution	Period
Temperature (°C)	Tmp	Copernicus Marine Environmental Monitoring Service website(http://marine.copernicus.eu/): "GLOBAL_REANALYSIS_PHY_001_031"	0.25°	Monthly average	10 years (12/16/2009 – 12/16/2019)
Chlorophyll concentration (mg.m-3)	Chl	Copernicus Marine Environmental Monitoring Service website(http://marine.copernicus.eu/): "GLOBAL_MULTIYEAR_BGC_001_029"	0.25°	Monthly average	10 years (12/16/2009 – 12/16/2019)
Kinetic Energy ($m^2.s^{-2}$)	KE	Copernicus Marine Environmental Monitoring Service website(http://marine.copernicus.eu/): "GLOBAL_REANALYSIS_PHY_001_031"	0.25°	Monthly average	10 years (12/16/2009 – 12/16/2019)
Mixed Layer Depth (m)	MLD	Copernicus Marine Environmental Monitoring Service website(http://marine.copernicus.eu/): "GLOBAL_REANALYSIS PHY_001_031"	0.25°	Monthly average	10 years (12/16/2009 – 12/16/2019)
Salinity	Sali	Copernicus Marine Environmental Monitoring Service website(http://marine.copernicus.eu/): "GLOBAL_REANALYSIS_PHY_001_031"	0.25°	Monthly average	10 years (12/16/2009 – 12/16/2019)
Oxygen concentration (mmol.m-3)	Oxy	Copernicus Marine Environmental Monitoring Service website(http://marine.copernicus.eu/): "GLOBAL_MULTIYEAR_BGC_001_029"	0.25°	Monthly average	10 years (12/16/2009 – 12/16/2019)

Statistical analyses

From the environmental data, seasonal and monthly climatologies over 10 years (2009–2019) were produced. Data were compiled in a large matrix with the sites in rows and the environmental variables in columns. At each grid point, there is a combination of environmental variables averaged over 10 years (Figure 2). From these climatologies, regions with similar spatio-temporal dynamics of environmental parameters were defined using two different methodological approaches. All statistical analyses were performed using R 4.0.5 (R, 2021) and the maps were produced with the *MapCDFTemp* function in R. Graphical representations were created using the '*ggplot2*' package (Wickham, 2014).

The first approach integrates the temporal dynamics of environmental parameters in the delimitation of regions since the strong seasonality of certain factors is an important parameter to take into account in the regionalisation process. It takes into account surface environmental data and is based on monthly climatologies. This method consists of defining coherent regions in terms of environmental data by performing Principal Component Analyses (PCA) and then applying the K-Means method to the results. PCA is an ordination technique that aims to represent the link between objects (sites) and descriptors (variables) in a limited number of dimensions (Legendre and Legendre, 1998). The Variance Inflation Factor (VIF) was calculated to test for collinearity (Neter et al., 1983). K-means clustering (MacQueen, 1967) involves automatically partitioning a dataset into k groups using Euclidean distance and this was done using the '*kmeans()*' function from the 'stats' package. The dataset consists of sites in rows and variables in columns, with the variables corresponding to the significant principal component of the PCA conducted on all variables. The '*NbClust*' package in R (Charrad et al., 2015) was used to determine the optimal number of groups although adjustments were made to this number when the obtained regions were insufficient for detailing the study area. Figures representing the temporal evolution of each environmental parameter for each group were also produced.

The second approach involves conducting functional Principal Component Analyses (fPCA) (Berrendero et al., 2011) using the vertical profile of each environmental parameter and applying k-means clustering to the results, as in the first approach. The study focused on three depth ranges: 0–200m, 200–1000m and 0–1000m, to consider different vertical layers according to the vertical distribution and the nycthemeral migration patterns of pelagic organisms. This method is novel because it takes into account the vertical dimension to discriminate groups with similar vertical data profiles. fPCA were performed using the '*fda.oce*' R package (Pauthenet et al., 2018). The fPCA is conducted on a set of vertical profiles (temperature, salinity, oxygen concentration) at each grid point. The vertical data profiles are stored in a matrix Xi (depths x stations x variables) and Pi which is a vector of the different depths (Figure 2). These profiles are first smoothed into spline function bases due to the irregular depth intervals in the dataset and then summarised by the fPCA before applying the K-Means method, which uses the coordinates of the vertical profiles in the main plan of the fPCA (two first components). Maps illustrating the distribution of the groups and figures representing smoothed temperature, salinity and oxygen concentration profiles for each region were produced.

The average climate velocity is estimated over each region obtained, both in the epipelagic and in the mesopelagic areas. Climate velocities were computed as the ratio between the temperature trend and the temperature spatial gradient (Loarie et al., 2009). This computation is done over 50 years (2015–2065) using climate models from the Coupled Model Intercomparison Project 6 (CMIP6; Eyring et al., 2016; models used and computation as in Azarian et al., 2023), under the Shared-Socioeconomic Pathways (or SSP) 1-2.6 (high mitigation scenario) and 2-4.5 (modest mitigation scenario), which represent paths leading to an estimated global warming of respectively 1.8°C and 2.7 °C by the end of the century. Note that climate velocities are computed only based on temperature, as temperature is a main driver of species distribution and a key variable in the regionalisations. Given that these climate velocities are mostly directed south and that the regions identified appear mostly structured in latitudinal bands, a « climate residence time » (concept developed in Brito-Morales et al., 2018) can be derived for each region by computing the ratio between the region mean latitudinal extent and mean climate velocity. This metric can be interpreted as the time it would take for the temperature conditions to completely shift outside of the historical region.

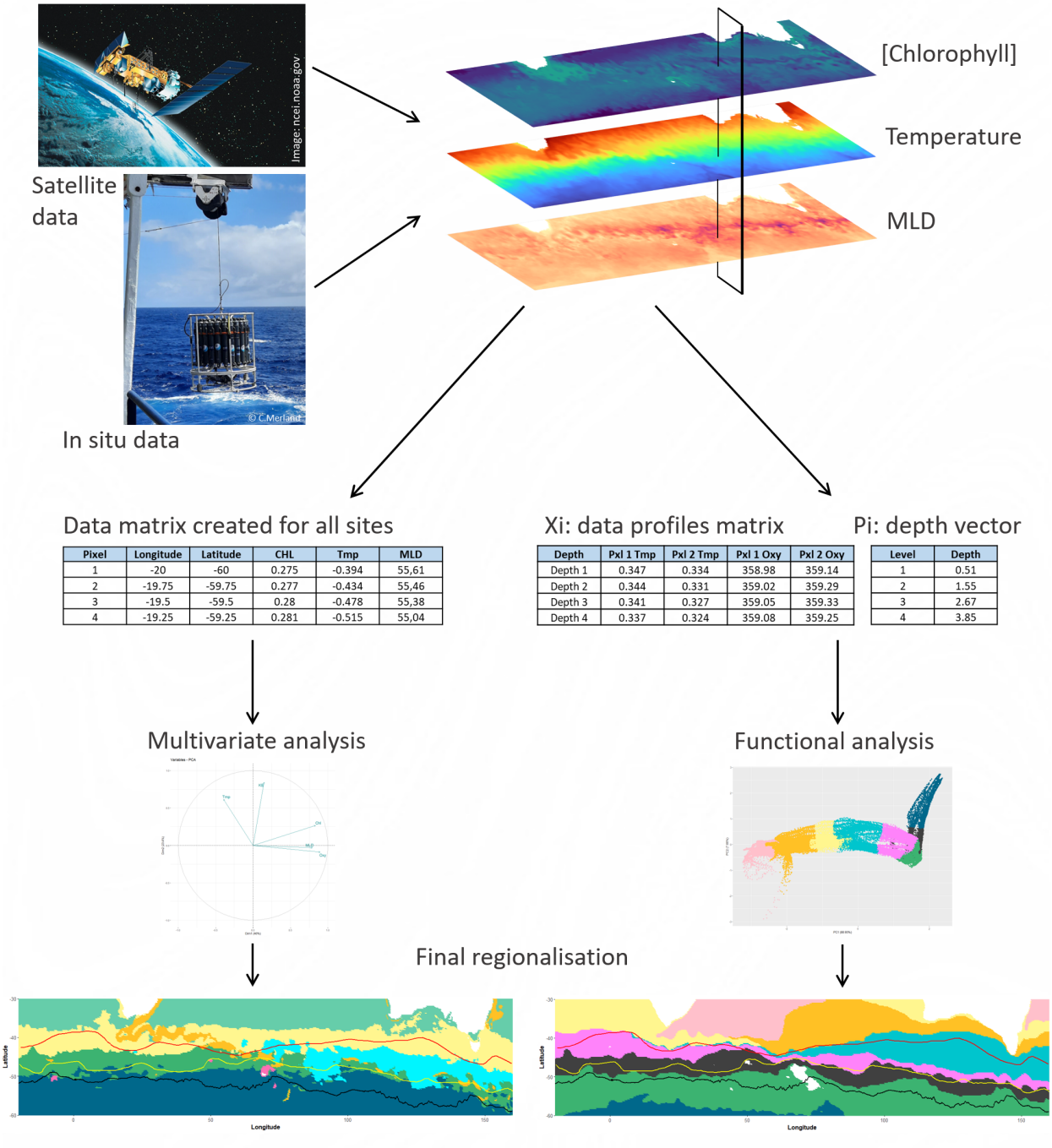

Pixel	Longitude	Latitude	CHL	Tmp	MLD
1	-20	-60	0.275	-0.394	55,61
2	-19.75	-59.75	0.277	-0.434	55,46
3	-19.5	-59.5	0.28	-0.478	55,38
4	-19.25	-59.25	0.281	-0.515	55,04

Depth	Pxl 1 Tmp	Pxl 2 Tmp	Pxl 1 Oxy	Pxl 2 Oxy
Depth 1	0.347	0.334	358.98	359.14
Depth 2	0.344	0.331	359.02	359.29
Depth 3	0.341	0.327	359.05	359.33
Depth 4	0.337	0.324	359.08	359.25

Level	Depth
1	0.51
2	1.55
3	2.67
4	3.85

Figure 2: Schematic representation of the methods used in this study.

Results

Multivariate analyses

The first approach identified seven regions that were consistent in term of spatiotemporal dynamics of environmental parameters (Figure 3):

From north to south, regions 5, 6, 1, and 3 are distinguished by different temperature and oxygen concentration ranges. The study area exhibits a latitudinal temperature gradient that decreases from north to south, coupled with an increase in oxygen concentration (Figures 4a and 4b).

Concerning the other groups, finer-scale regions stand out and are characterised by parameters with a strong seasonality. Region 4 is marked by strong winter mixing at depths (> 250 m between August and September) contrasting with shallower winter mixing layer depths ranging from 50 and 150 m at most of the other regions (Figure 4d). Region 2 is defined by high values of kinetic energy associated with the Agulhas Current and Agulhas Return Current, while the other regions globally exhibit lower mesoscale activity (Figure 4e). Finally, region 7 is characterised by high chlorophyll concentrations and a different temporal dynamic compared to the others (Figure 4c). This region, located around the Crozet archipelago, Kerguelen and Heard Islands, is probably differentiated by island effects. Chlorophyll concentration is highest between late spring and summer with a peak in November.

Furthermore, the different fronts have been superimposed on this regionalisation map but we note that they do not correspond to the transition between the identified regions. Table 2 summarises the names and main characteristics of each region identified by the multivariate method.

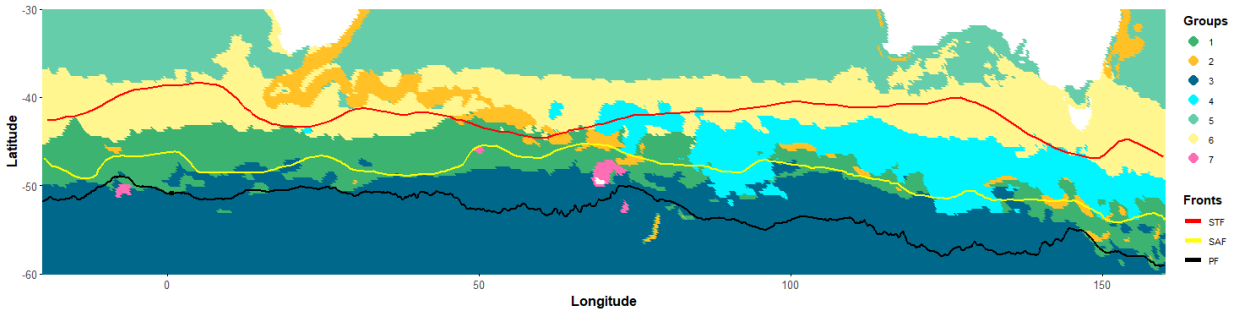

Figure 3: Mapping of regions identified by the K-Means method, with similar spatiotemporal dynamics of environmental parameters. Subtropical Front (STF), Subantarctic Front (SAF) and Polar Front (PF) are also mapped.

Table 2: Names and characteristics of the regions identified by the multivariate analysis.

Regions	Name	Characteristics
1	Medium/low temperature and medium/high O2 concentration region	5°C < Tmp < 8°C ; 300 mmol.m^{-3} < [Oxy] < 325 mmol.m^{-3}
2	Turbulent region	KE > 0.09 m^2.s-^{2}
3	Low temperature and high O2 concentration region	1°C < Tmp < 4°C ; [Oxy] > 325 mmol.m^{-3}
4	High MLD region	50m < MLD < 250m
5	High temperature and low O2 concentration region	16°C < Tmp < 21°C ; [Oxy] < 250 mmol.m^{-3}
6	Medium/high temperature and medium/low O2 concentration region	12°C < Tmp < 16°C ; 260 mmol.m^{-3} < [Oxy] < 275 mmol.m^{-3}
7	Productive region	0.60 mg.m^{-3} < [Chl] < 1.25 mg.m^{-3}

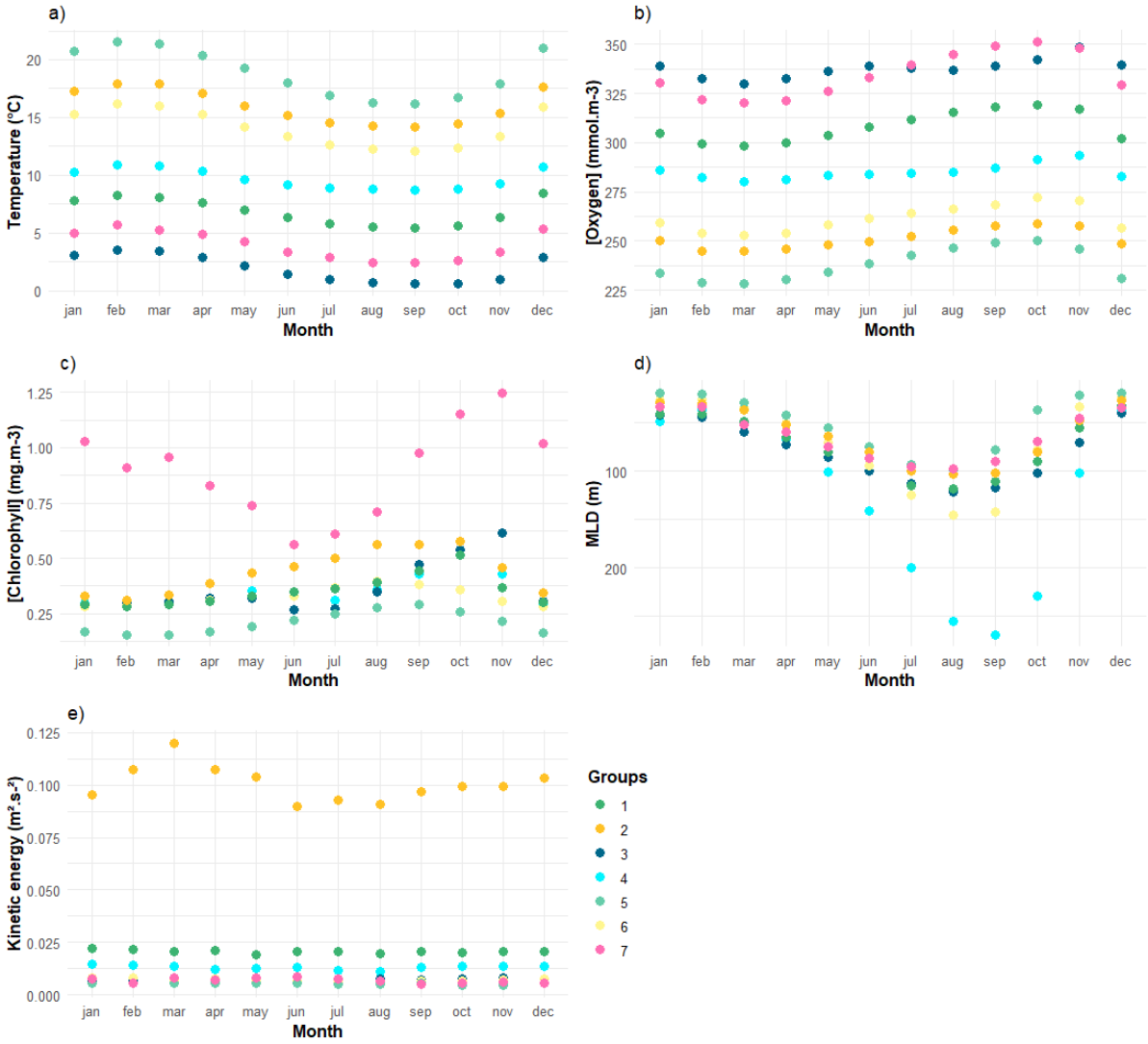

Figure 4: Temporal evolution of a) temperature (°C), b) oxygen concentration (mmol.m-3), c) chlorophyll concentration (mg.m-3), d) MLD (m) and e) kinetic energy (m^2. s^{-2}) for each region.

Functional analyses

The second approach identified seven distinct regions characterised by similar vertical data profiles for the 'epipelagic' (0–200 m) analysis (Figure 5a). For the 'mesopelagic' (200–1000 m) and 'epi+mesopelagic' (0–1000 m) analyses, an additional region was identified (Figures 5b and 5c) in the south-east Atlantic Ocean extending over a narrow latitudinal band between 38 and 45°E in the Indian sector of the Southern Ocean. For all analyses, a decreasing gradient in temperature and salinity and an increasing gradient in oxygen concentration from north to south are observed. Within the Antarctic and Subantarctic zones, the groups appear to be circumpolar and are more or less the same between the different analyses except the region 1, that extend over a larger latitudinal area for epipelagic analysis than in the other two, where it is more restricted. Furthermore, subdivisions are observed in the Subtropical Zone with a separation between the eastern and the western parts of the South Indian Ocean. This east/west distinction is starker in the mesopelagic analysis as well as the one integrating the two depth ranges. Differences in temperature and oxygen concentrations seem to explain this separation (Figure 6).

We observe that the Polar Front marks the boundary between the epipelagic Antarctic regions 1 and 2, the Subantarctic Front is at the boundary between epipelagic regions 2 and 3 in particular west of the Kerguelen Plateau and the Subtropical Front seems to follow the boundary between the epipelagic Subantarctic region 4 and subtropical region 5. However, those fronts no longer match regions' boundaries in the mesopelagic area.

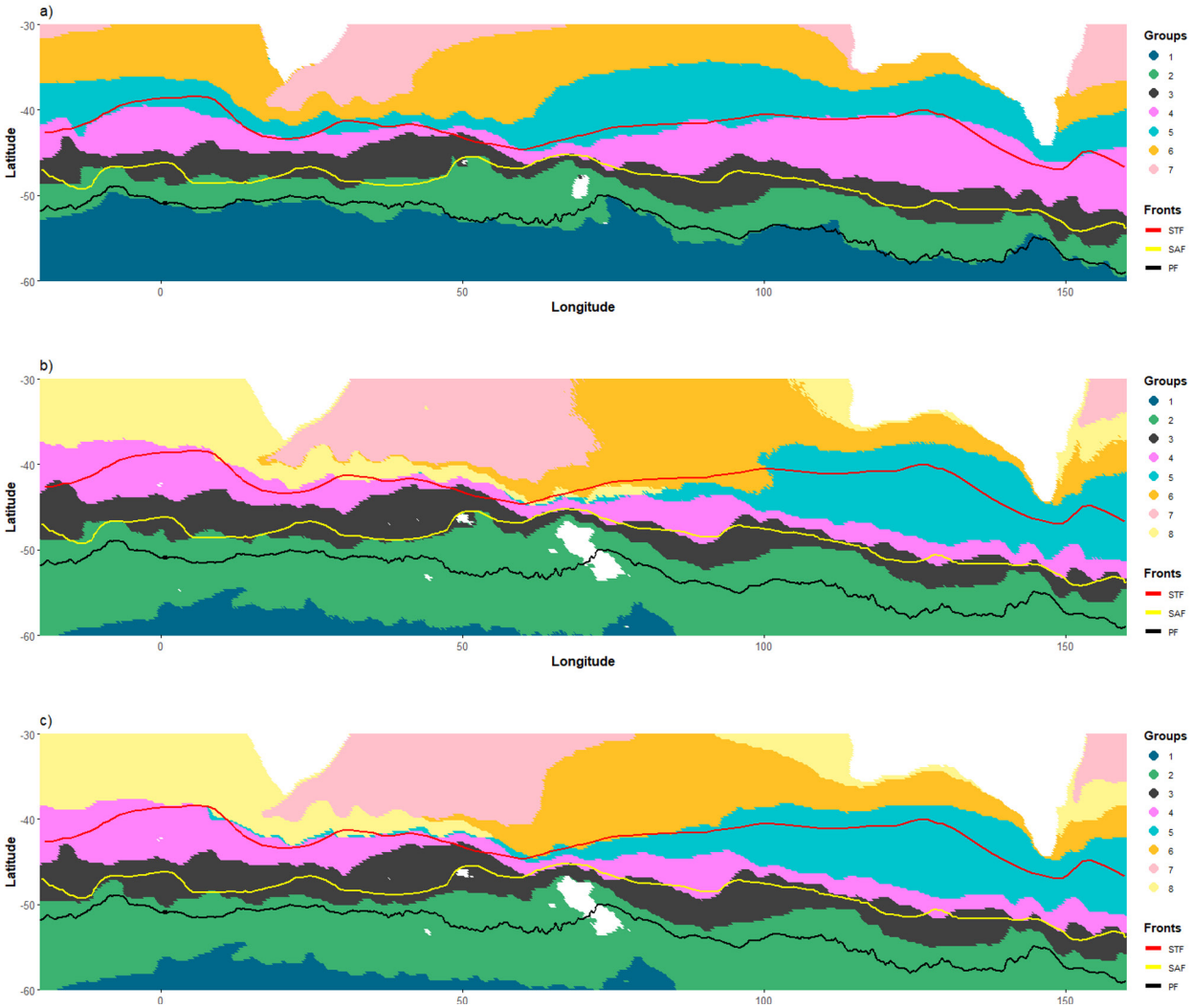

Figure 5: Mapping of regions identified by the K-Means method with similar vertical profiles of temperature, salinity, and oxygen concentration for the a) 'epipelagic', b) 'mesopelagic', and c) 'epi + mesopelagic' analysis. Subtropical Front (STF), Subantarctic Front (SAF) and Polar Front (PF) are also mapped.

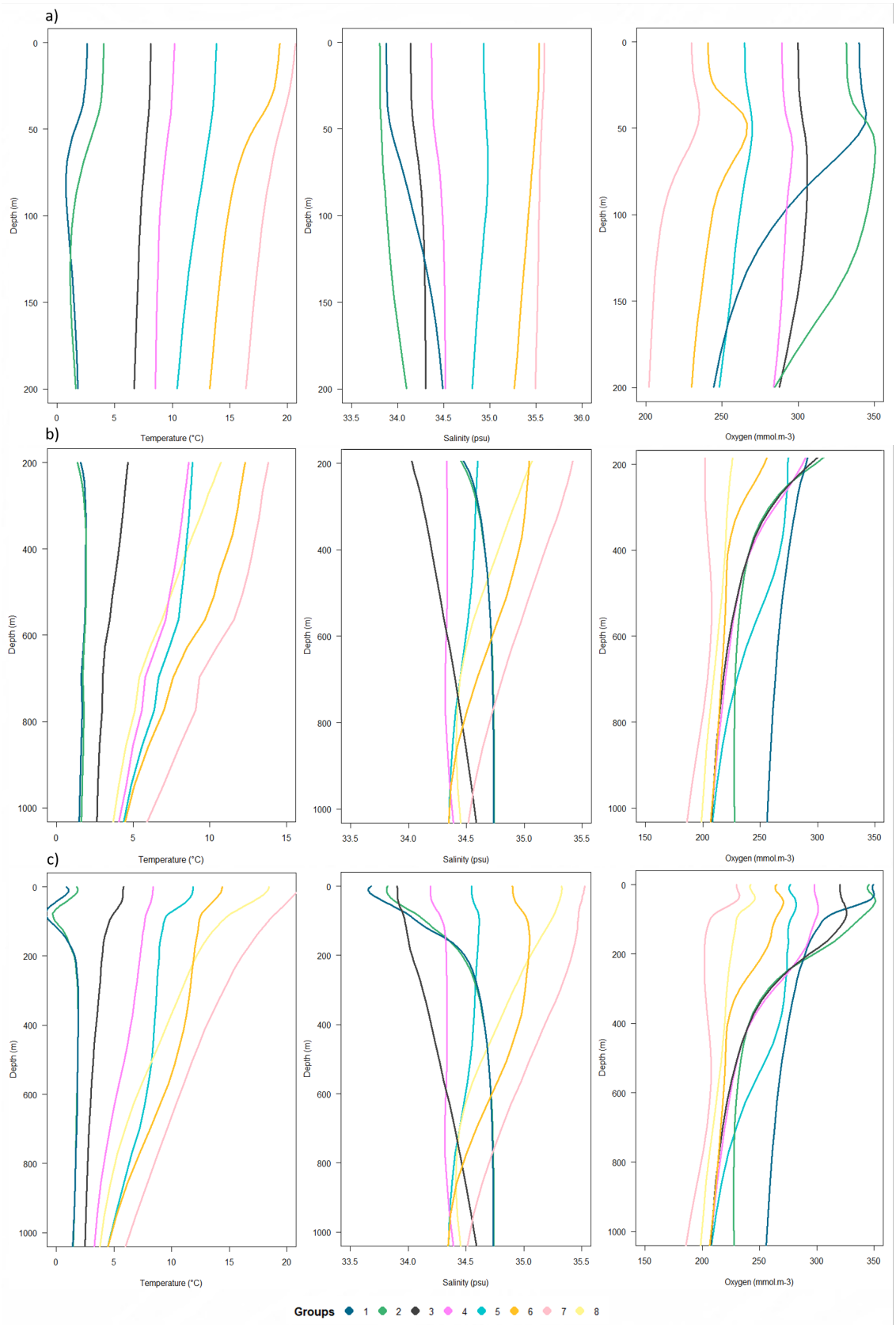

Figure 6: Representation of the smoothed vertical profiles of temperature (°C), salinity (psu) and oxygen concentration (mmol.m-3) of the different regions for the a) 'epipelagic', b) 'mesopelagic', and c) 'epi + mesopelagic' analysis.

Climate velocities over the epipelagic and mesopelagic regions

Climate velocities over the regions obtained using the functional approach are faster under SSP2-4.5 than SSP1-2.6 and ranges between 20.7 and 42.7 km/decade in the epipelagic and between 26.3 and 73.7 km/decade in the mesopelagic under SSP2-4.5 (Figure 7). Climate velocities in the mesopelagic regions tend to be faster than in the epipelagic ones under both scenarios, in particular in the subtropical regions 5 and 6 (around twice as fast). Although the epipelagic and mesopelagic regions found tend to overlap, they do not overlap systematically and by definition do not represent exactly the same characteristics. Still, climate velocities in epipelagic regions tend to decrease from south to north and the highest climate velocities are found in the east subtropical mesopelagic regions under both scenarios. This metric can also be put in relation with the latitudinal extent of the region to evaluate its climate residence time. In the mesopelagic, all regions have a climate residence time shorter than a century except for the Antarctic region 2 and the Subtropical region 7, mostly because they have a larger latitudinal extent. For regions with similar climate velocities, those with limited latitudinal extent may be the most impacted by climate change.

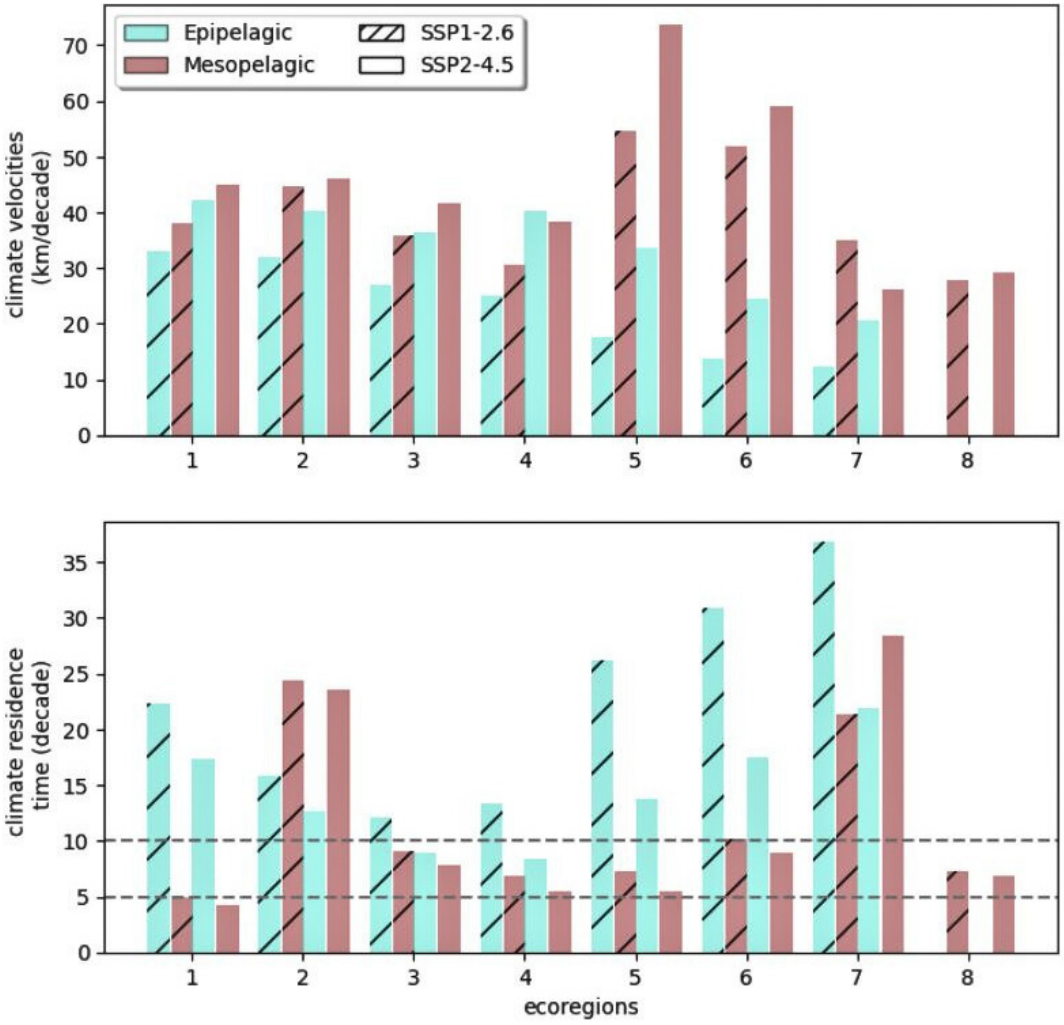

Figure 7: a) Average climate velocity and b) climate residence time over each epipelagic (blue) and mesopelagic (brown) regions determined with the second regionalisation approach, using climate models over 20°E–120°E 60°S–30°S as in Azarian et al., 2023, under SSP1–2.6 (hatched) and SSP2–4.5 (not hatched). Dashed horizontal grey lines for climate residence time at 5 and 10 decades are provided to help with the readability of the figure highlighting key orders of magnitude.

Discussion

The regionalisations we propose here incorporate a broad latitudinal gradient (30°S – 60°S) and include several different oceanic zones (Subtropical Zone, Subantarctic Zone, Polar Frontal Zone and Antarctic Zone). To achieve these regionalisations, two methodological approaches were employed, one focusing on surface environmental data, and the other considering space-time dimensions through their vertical profiles.

Surface regionalisation at scales relevant for conservation

Different regions were identified through multivariate analyses. In terms of surface, the four largest regions (5, 6, 1 and 3) were distinguished by different temperature and oxygen concentration ranges. Consequently, the studied geographical area exhibits a decreasing latitudinal gradient of temperature and increasing oxygen concentration from north to south with a circumpolar distribution previously described (Park et al., 1991). The other regions depict environmental features exhibiting a strong seasonality.

The region of high MLD (region 4) extends over a broad longitudinal band mainly between 70°E and 160°E and is characterised by a deep mixed layer in winter. This deepening is particularly important in August and September, where depths of nearly 400 m can be reached. It is also observed in other regions, but is less pronounced. These areas of high winter MLD have been previously identified in several studies (Dong et al., 2007; Sallée et al., 2013; Toyoda et al., 2015) and Buongiorno Nardelli et al. (2017) showed that the greatest depths are found between June and October in the north of the ACC. These areas are also considered to be the main regions of Subantarctic Mode Waters (SAMW) formation (Buongiorno Nardelli et al., 2017). Furthermore, region 4 is also characterised by intermediate temperature and oxygen concentration ranges and low kinetic energy.

The turbulent region (region 2) is characterised by high kinetic energy values associated with the Agulhas Current and the Agulhas Return Current on a longitudinal band located between 10°E and 50°E. Specifically, the Agulhas Current follows the continental shelf break of southeastern Africa until it reaches the southern tip of the continent. At this point, the Agulhas Return Current takes over (Lutjeharms and Ansorge, 2001) and potentially extends to 72°E according to Belkin and Gordon's study (1996). These two regions thus represent the highly energetic zones of the Southern Indian Ocean. This intense circulation probably plays a crucial role in transporting nutrients from the African coasts and shelf to the southern and eastern open ocean areas and more particularly towards the Subantarctic islands. It is possible that this intense circulation supports phytoplankton production and may inject communities with an affinity for warmer waters towards the Subantarctic region. This region is also characterised by high temperature ranges and low oxygen concentrations.

The productive region (region 7) is located around the Crozet archipelago, Kerguelen and Heard Islands. It corresponds to the most productive zones and is probably marked by island effects. Chlorophyll concentration is highest during the end of spring with a peak observed in November. Indeed, temporal variations in chlorophyll concentration in the Southern Ocean are due to phytoplankton blooms, while their locations are influenced by iron enrichment from the islands and their shelves (Blain et al., 2001; Sokolov and Rintoul, 2007; Graham et al., 2015).

Accounting for vertical structure: epipelagic and mesopelagic regionalisations

The functional method identified seven distinct regions in the 'epipelagic' analysis while eight regions were identified in the 'mesopelagic' analysis and in the one covering both depth ranges. The different regions are distinguished by distinct temperature, salinity and oxygen concentration ranges revealing a latitudinal structuring as observed in multivariate analyses. Notably, further subdivisions are visible in the Subtropical Zone with a clear separation between the eastern and western parts of the South Indian Ocean (regions 6 and 7). This separation could potentially be attributed to temperature differences. Indeed, several studies (Behera and Yamagata, 2001; Suzuki et al., 2004; Morioka et al., 2010) have documented temperature differences between the eastern and western parts of the South Indian Ocean. This pattern could be explained by the presence of the Agulhas Return Current which transports warm water currents from the low latitudes of the Indian Ocean via the Agulhas Current. Moreover, the western part and

the southern part of region 7 seems to overlap well with the position of the Agulhas Current and the Agulhas Return Current respectively. The Agulhas effect is also visible to the south of South Africa. This corresponds to relatively warm and saline waters flowing from the Indian Ocean to the Atlantic Ocean via large anticyclonic Agulhas rings, cyclonic eddies and direct inflow (Schmidt et al., 2021). This pattern clearly highlights that region 7 is under the influence of these two currents. In addition, there are differences in terms of extension to the east for this region, depending on the different depth ranges studied. It extends particularly further along the longitude (70°E) for the mesopelagic analysis as well as for the analysis that integrates the two depth ranges, whereas it does not extend beyond 50°E for the epipelagic analysis. The presence of a subduction zone could explain why the region 7 is larger in the mesopelagic analysis (Sallée et al., 2010).

The analysis carried out on the mesopelagic layer and that which integrates the two deep layers has revealed the existence of an additional region (region 8), located in the south-east Atlantic Ocean and extending over a restricted latitudinal band in the Indian sector of the Southern Ocean. This region is characterised by lower temperature and salinity profiles, and higher oxygen concentration profiles. These characteristics are probably due to the presence of the Benguela upwelling located off the coast of southwest Africa, characterised by colder and more oxygenated waters.

We also observed that region 1 extends over a larger latitudinal zone in the epipelagic analysis than in the other two. This region is mainly distinguished from region 2 by different oxygen concentrations. This suggests that the distinctions are more pronounced in the epipelagic zone than at depth in terms of oxygen concentrations.

Complementarity of the two methods

The two methods used in this study are complementary in terms of depicted spatial and temporal patterns. The first method, while constrained to surface data, offers the advantages of integrating a diverse set of environmental parameters. Through this method, it is possible to delimit the zone latitudinally according to the existing gradients of temperature and oxygen concentration. It also allowed the identification of smaller regions, at scales relevant for conservation, such as highly energetic or highly productive regions together with their seasonal cycles. The functional analysis integrates fewer parameters, but it enables the delineation of areas by considering multiple depth ranges and not just surface data. This provides additional information on the latitudinal delimitation of regions based on 3-dimensional gradients in temperature, salinity and oxygen concentration. Notably, it reveals an additional subdivision in the Subtropical Zone with a distinction between the eastern and western parts of the South Indian Ocean.

Current bioregionalisation studies coupled with physical regionalisation do not take into account the 3D structuring of species assemblages. Although complementary, the second approach would therefore be better suited to a bioregionalisation approach by integrating species abundance data, since it incorporates data at depth. It would also allow assessment whether this east/west subdivision can influence the structure of zooplankton assemblages in this area. Variations in assemblages at the same latitudes have already been observed in the Subtropical Zone between the western and eastern transects sampled by the R/V *Marion Dufresne II* during the REPCCOAI surveys in 2017, 2018 and 2019 (Merland and Thellier, 2025). These differences may be due to the influence of Agulhas Return Current, which could possibly transport species from warmer tropical waters to the western part of the South Indian Ocean potentially explaining the observed distinctions in assemblages at similar latitudes. Indeed, particular zooplanktonic species (notably siphonophores and euphausiids) found in the warm waters north of the Crozet Archipelago have been also observed in the Agulhas Current (Gibbons et al., 1995; Gibbons and Thibault-Botha, 2002), possibly transported by the Agulhas Return Current to reach Subantarctic latitudes.

We observed that the ACC fronts do not match either the boundaries between the different regions defined with the first approach, or the boundaries between mesopelagic regions obtained with the second approach. However, the fronts overlap well with the epipelagic regions of the second method which is consistent with fronts mostly characterising (sub)surface physical conditions. Although fronts are useful as indicators of water masses boundaries in a bioregionalisation approach, they remain

insufficient in explaining deeper 3D structuring of pelagic communities as a whole.

Finally, this functional approach can be particularly useful for conservation under climate change as it contributes to better characterising pelagic habitats that may be impacted differently at depth. The Southern Indian Ocean is projected to undergo significant warming (0.29°C warming in 2021–2040 under a modest mitigation scenario), especially at Subantarctic latitudes (Azarian et al., 2023). However, the velocities of change can differ between the epipelagic and mesopelagic zones. Indeed, climate models project faster climate velocities of temperature in the mesopelagic compared to the epipelagic at the end of the century, especially north of the Subtropical Front (Azarian et al., 2023), which is also observed here for the coming 50 years over subtropical regions 5 and 6. This difference could lead in some cases to habitat shearing for species that migrate throughout the water column. In less than a century, the temperature conditions of most of the mesopelagic regions identified could shift outside their historical boundaries, regardless of the emission scenario. In that context, identifying the vertical structure of species habitats is key: to understand the mechanisms driving zooplankton assemblages at depth can provide insights on how they may be impacted by climate change.

In further studies, it would be valuable to explore variations in abundance and diversity among these distinct physical and biochemical regions but also conducting habitat models to discern the environmental parameters influencing assemblage structure. As recently demonstrated with acoustic three-dimensional data (Izard et al. 2024), it would be useful to perform a single oceanographic functional cluster analyses which include temporal and spatial modes of variability. Such an approach could unveil the connections between these assemblages and environmental parameters, allowing predictions about their potential future distribution.

Acknowledgements

The authors acknowledge Aviso, ACRI-ST and the European Copernicus Marine Environment Monitoring Service for the production and the delivery of environmental data. This project was funded by ASOC in 2022. This paper is a contribution to the pelagic ecoregionalisation of the Subantarctic zone (Makhado et al., 2023) and the PHOCIS project (Pelagic high seas ecoregionalisation of the Indian Subantarctic). The REPCCOAI surveys (Responses of the Pelagic Ecosystem to Climate Change in the Southern and South Indian Ocean) was directed by P. Koubbi and J.-Y. Toullec (Roscoff Biological Station). These surveys were supported by the French oceanographic fleet, the CNRS Antarctic Workshop Zone, the CNES KERTREND-SAT OSTST project led by Francesco d'Ovidio (LOCEAN), the European MESOPP H2020 programme and the TAAF National Nature Reserve programmes.

References

Azarian, C., L. Bopp, A. Pietri, J.B. Sallée and F. d'Ovidio. 2023. Current and projected patterns of warming and marine heatwaves in the Southern Indian Ocean. *Prog. Oceanogr.*, 2015: 103036. https://doi.org/10.1016/j.pocean.2023.103036.

Behera, S. K. and T. Yamagata. 2001. A dipole mode in the tropical Indian Ocean. *Geophys. Res. Lett.*, 28(2): 327-330. https://doi.org/10.1029/2000GL011451.

Belkin, I. M. and A. L Gordon. 1996. Southern Ocean fronts from the Greenwich meridian to Tasmania. *J. Geophys. Res. Oceans*, 101(C2), 3675–3696. https://doi.org/10.1029/95JC02750.

Berrendero, J. R., A. Justel and M. Svarc. 2011. Principal components for multivariate functional data. *Comput. Stat. Data Anal.*, 55(9): 2619–2634. https://doi.org/10.1016/j.csda.2011.03.011.

Blain, S., P. Tréguer, S. Belviso, E. Bucciarelli, M. Denis, S. Desabre, M. Fiala, V.M. Jézéquel, J. Le Fèvre, P. Mayzaud, J.-C. Marty and S. Razouls. 2001. A biogeochemical study of the island mass effect in the context of the iron hypothesis: Kerguelen Islands, Southern

Ocean. *Deep-Sea Res. I: Oceanogr. Res. Pap.*, 48(1): 163-187. https://doi.org/10.1016/S0967-0637(00)00047-9.

Brito-Morales, I., D.S. Schoeman, J.G. Molinos, M.T. Burrows, C.J. Klein, N. Arafeh-Dalmau, K. Kaschner, C. Garilao, K. Kesner-Reyes and A.J. Richardson. 2020. Climate velocity reveals increasing exposure of deep-ocean biodiversity to future warming. *Nat. Clim. Chang.*, 10 (6): 576–581. https://doi.org/10.1038/s41558-020-0773-5.

Buongiorno Nardelli, B., S. Guinehut, N. Verbrugge, Y. Cotroneo, E. Zambianchi, and D. Iudicone. 2017. Southern Ocean mixed-layer seasonal and interannual variations from combined satellite and in situ data. *J. Geophys. Res. Oceans*, 122(12): 10042-10060. https://doi.org/10.1002/2017JC013314.

Charrad, M., N. Ghazzali, V. Boiteau and A.N. Maintainer. 2015. *Determining the Best Number of Clusters in a Data Set*.

Dong, S., S.T. Gille and J. Sprintall. 2007. An assessment of the Southern Ocean mixed layer heat budget. *J. Climate*, 20: 4425-4442. https://doi.org/10.1175/JCLI4259.1.

Eyring, V., S. Bony, G.A. Meehl, C.A. Senior, B. Stevens, R.J. Stouffer and K.E. Taylor. 2016. Overview of the Coupled Model Intercomparison Project Phase 6 (CMIP6) experimental design and organization. *Geosci. Model Dev.*, 9 (5), 1937–1958. https://doi.org/10.5194/gmd-9-1937-2016.

Ferry, N., L. Parent, G. Garric, B. Barnier and N.C. Jourdain. 2010. Mercator global Eddy permitting ocean reanalysis GLORYS1V1: Description and results. *Mercator-Ocean Quarterly Newsletter*, 36: 15–27.

Godet, C., M. Robuchon, B. Leroy, C. Cotté, A. Baudena, O. Da Silva, S. Fabri-Ruiz, C. Lo Monaco, S. Sergi and P. Koubbi. 2020. Matching zooplankton abundance and environment in the South Indian Ocean and Southern Ocean. *Deep-Sea Res. I: Oceanogr. Res. Pap.*, 163: 103347. https://doi.org/10.1016/j.dsr.2020.103347.

Graham, R.M., A.M. De Boer, E. van Sebille, K.E. Kohfeld and C. Schlosser. 2015. Inferring source regions and supply mechanisms of iron in the Southern Ocean from satellite chlorophyll data. *Deep-Sea Res. I: Oceanogr. Res. Pap.*, 104: 9–25. https://doi.org/10.1016/j.dsr.2015.05.007.

Grant, S., A. Constable, B. Raymond and S. Doust. 2006. Bioregionalisation of the 628 Southern Ocean. Hobart.

Gibbons, M.J., M. Barange and L. Hutchings. 1995. Zoogeography and diversity of euphausiids around southern Africa. *Mar. Biol.*, 123: 257–268. https://doi.org/10.1007/BF00353617.

Gibbons, M.J. and D. Thibault-Botha. 2002. The match between ocean circulation and zoogeography of epipelagic siphonophores around southern Africa. *JMBA*, 82(5): 801–810. https://doi.org/10.1017/S0025315402006161.

Izard, L., N. Fonvieille, C. Merland, P. Koubbi, D. Nerini, J. Habasque, A. Lebourges-Dhaussy, C. Lo Monaco, G. Roudaut, F. D'ovidio, J.-B. Charrassin and C. Cotté. 2024. Decomposing acoustic signal reveals the pelagic response to a frontal system between oceanic domains. *J. Mar. Syst.*, 243: 103951. https://doi.org/10.1016/j.jmarsys.2023.103951.

Koubbi, P., M. Moteki, G. Duhamel, A. Goarant, P.-A. Hulley, R. O'Driscoll, T. Ishimaru, P. Pruvost, E. Tavernier and G. Hosie. 2011. Ecoregionalization of myctophid fish in the Indian sector of the Southern Ocean: Results from generalized dissimilarity models. *Deep-Sea Res. II: Top. Stud. Oceanog.*, 58(1–2): 170–180. https://doi.org/10.1016/j.dsr2.2010.09.007.

Legendre, P.L. and L. Legendre. 1998. *Numerical ecology*. Elsevier, Amsterdam: 852 pp.

Loarie, S.R., P.B. Duffy, H. Hamilton, G.P. Asner, C.B. Field and D.D. Ackerly. 2009. The velocity of climate change. *Nature*, 462 (7276): 1052–1055. https://doi.org/10.1038/nature08649.

Longhurst, A. 2007. *Ecological Geography of the Sea*. Academic Press, London: 560 pp.

Lutjeharms, J.R.E. and I.J. Ansorge. 2001. The Agulhas return current. *J. Mar. Syst.*, 30(1-2): 115-138. https://doi.org/10.1016/S0924-7963(01)00041-0.

MacQueen, J.B. 1967. Kmeans Some Methods for classification and Analysis of Multivariate Observations. *5th Berkeley Symp. Math. Stat. Probab.*, 1967(1): 281–297.

Makhado, A.B., A. Lowther, P. Koubbi, I. Ansorge, C. Brooks, C. Cotté, R. Crawford, S. Dlulisa, F. d'Ovidio, S. Fawcet, D. Freeman, S. Grant, J. Huggett, M. Hindell, P.A. Hulley, S. Kirkman, T. Lamont, M. Lombard, M.J. Masothla, M.-A. Lea, W.C. Oosthuizen, F. Orgeret, R. Reisinger, T. Samaai, S. Sergi, K. Swadling, S. Somhlaba, A. Van de Putte, C. Von de Meden and D. Yemane. 2019. Expert Workshop on Pelagic Spatial Planning for the eastern subantarctic region (Domains 4, 5 and 6). Document *SC-CAMLR-38/BG/29*. CCAMLR, Hobart, Australia: 71 pp.

Merland, C. and M. Thellier. 2025. Macrozooplankton from Crozet to Kerguelen and Subtropical Southern Indian Ocean. *CCAMLR Science*, 25: 99–116.

Morioka, Y., T. Tozuka and T. Yamagata. 2010: Climate variability in the southern Indian Ocean as revealed by self-organizing maps. *Clim. Dyn.*, 35: 1059–1072. https://doi.org/10.1007/s00382-010-0843-x.

Neter, J., W. Wasserman and M.H. Kutner. 1983. Variance inflation factors and other methods of detecting multicollinearity. *Applied Linear Regression Models*, 390–392.

Park Y.-H., L. Gamberoni and E. Charriaud. 1991. Frontal structure and transport of the Antarctic Circumpolar Current in the south Indian Ocean sector, 40–80°E. *Mar. Chem.*, 35(1–4): 45–62.

Park, Y.-H. and I. Durand. 2019. Altimetry-derived antarctic circumpolar current fronts. *SEANOE*. https://doi.org/10.17882/59800.

Pauthenet, E., F. Roquet, G. Madec, C. Guinet, M. Hindell, C.R. McMahon, R. Harcourt and D. Nerini. 2018. Seasonal meandering of the Polar Front upstream of the Kerguelen Plateau. *Geophys. Res. Lett.*, 45(18): 9774–9781. https://doi.org/10.1029/2018GL079614,

Raymond, B. 2014. Pelagic regionalisation. In: De Broyer, C., P. Koubbi, H. Griffiths, B. Danis, B. David, S. Grant, J. Gutt, C. Held, G. Hosie, F. Huettmann, A. Post, B. Raymond, Y. Ropert-Coudert and A. van de Putte (eds). The CAML/SCAR-MarBIN Biogeographic Atlas of the Southern Ocean. *Scientific Committee on Antarctic Research*, Cambridge, pp. 418–421.

Reygondeau, G., L. Guidi, G. Beaugrand, S.A. Henson, P. Koubbi, P., B.R. MacKenzie, T.T. Sutton, M. Fioroni and O. Maury. 2018. Global biogeochemical provinces of the mesopelagic zone. *J. Biogeogr.*, 45(2): 500-514. https://doi.org/10.1111/jbi.13149.

Reygondeau, G., W.W.L. Cheung, C.C.C. Wabnitz, V.W.Y. Lam, T. Frölicher and O. Maury. 2020. Climate change-induced emergence of novel biogeochemical provinces. *Front. Mar. Sci.*, 7: 657. https://doi.org/10.3389/fmars.2020.00657.

Sallée, J. B., K. Speer, S. Rintoul and S. Wijffels. 2010. Southern Ocean thermocline ventilation. *J. Phy. Oceanogr.*, 40(3): 509–529.

Sallée, J. B., E. Shuckburgh, N. Bruneau, A.J. Meijers, T.J. Bracegirdle and Z. Wang. 2013. Assessment of Southern Ocean mixed-layer depths in CMIP5 models: Historical bias and forcing response. *J. Geophys. Res.: Oceans*, 118(4), 1845–1862. https://doi.org/10.1002/jgrc.20157.

Schmidt, C., F.U. Schwarzkopf, S. Rühs and A. Biastoch. 2021. Characteristics and robustness of Agulhas leakage estimates: an inter-comparison study of Lagrangian methods. *Ocean Sci.*, 17(4) : 1067–1080. https://doi.org/10.5194/os-17-1067-2021.

Sokolov, S. and S.R. Rintoul. 2007. On the relationship between fronts of the Antarctic Circumpolar Current and surface chlorophyll concentrations in the Southern Ocean. *J. Geophys. Res.: Oceans*, 112(C7). https://doi.org/10.1029/2006JC004072.

Suzuki, R., S.K. Behera, S. Iizuka and T. Yamagata. 2004. Indian Ocean subtropical dipole simulated using a coupled general circulation model. *J. Geophys. Res.*, 109(C9). https://doi.org/10.1029/2003JC001974.

Testa, G., A. Piñones and L.R. Castro. 2021. Physical and Biogeochemical Regionalization of the Southern Ocean and the CCAMLR Zone

48.1. *Front. Mar. Sci.*, 8: 592378. https://doi.org/10.3389/fmars.2021.592378.

Toyoda, T., Y. Fujii, T. Kuragano et al. 2015. Intercomparison and validation of the mixed layer depth fields of global ocean syntheses. *Clim. Dyn.*, 49 : 753–773. https://doi.org/10.1007/s00382-015-2637-7.

Vidard, A., E. Rémy and E. Greiner. 2011. *Sensitivity analysis through adjoint method: application to the GLORYS reanalysis*.

Vierros, M., I. Cresswell, E. Escobar B., J. Rice and J. Ardron. 2009. *GOODS (Global Open Oceans and Deep Seabed) Biogeographic classification*.

Wickham, M.H. 2014. *Package 'ggplot2'*.